This study was supported by Grants-in-Aid for Scientific Research from the Ministry of Education, Culture, Sports, Science, and Technology, Japan (25670155, 23500384, 23500384); the grant from the Ministry of Health, Labor, and Welfare (2013–2017, 2014–2016); Scientific Research on Innovative Areas, a MEXT Grant-in-Aid Project 2012–2013; Strategic Research Foundation at Private Universities (2013–2017); the grant from the Human Science Foundation (2012–2013); and a grant from the Uehara Memorial Foundation.

Author Contributions

A.K., A.F., T.Y., Y.N., Y.H., T.S., Y.I., M.K., O.S., S.A, H.R., A.K., L.P.T, M.S., T.F., H.T. performed experiments. K.K., Y.N., H.K., K.M., T.N., J.M. T.T., H.T. analyzed data. T.T., H.T. wrote the manuscript.

Conflicts of Interest

No conflicts of interest, financial or otherwise, are declared by the author(s).

References

1. Sonkusare, S.K.; Kaul, C.L.; Ramarao, P. Dementia of Alzheimer's disease and other neurodegenerative disorders—Memantine, a new hope. *Pharmacol. Res.* **2005**, *51*, 1–17.
2. Lipton, S.A. Paradigm shift in neuroprotection by NMDA receptor blockade: Memantine and beyond. *Nat. Rev. Drug Discov.* **2006**, *5*, 160–170.
3. Szczurowska, E.; Mares, P. NMDA and AMPA receptors: Development and status epilepticus. *Physiol. Res.* **2013**, *62* (Suppl. 1), S21–S38.
4. Kupper, J.; Ascher, P.; Neyton, J. Probing the pore region of recombinant N-methyl-D-aspartate channels using external and internal magnesium block. *Proc. Natl. Acad. Sci. USA* **1996**, *93*, 8648–8653.
5. Wong, E.H.; Kemp, J.A.; Priestley, T.; Knight, A.R.; Woodruff, G.N.; Iversen, L.L. The anticonvulsant MK-801 is a potent N-methyl-D-aspartate antagonist. *Proc. Natl. Acad. Sci. USA* **1986**, *83*, 7104–7108.
6. Hansen, R.A.; Gartlehner, G.; Lohr, K.N.; Kaufer, D.I. Functional outcomes of drug treatment in Alzheimer's disease: A systematic review and meta-analysis. *Drugs Aging* **2007**, *24*, 155–167.
7. Uemura, T.; Lee, S.J.; Yasumura, M.; Takeuchi, T.; Yoshida, T.; Ra, M.; Taguchi, R.; Sakimura, K.; Mishina, M. Trans-synaptic interaction of GluRdelta2 and Neurexin through Cbln1 mediates synapse formation in the cerebellum. *Cell* **2010**, *141*, 1068–1079.
8. Matsuda, K.; Miura, E.; Miyazaki, T.; Kakegawa, W.; Emi, K.; Narumi, S.; Fukazawa, Y.; Ito-Ishida, A.; Kondo, T.; Shigemoto, R.; *et al.* Cbln1 is a ligand for an orphan glutamate receptor delta2, a bidirectional synapse organizer. *Science* **2010**, *328*, 363–368.
9. Kakegawa, W.; Miyoshi, Y.; Hamase, K.; Matsuda, S.; Matsuda, K.; Kohda, K.; Emi, K.; Motohashi, J.; Konno, R.; Zaitsu, K.; *et al.* D-Serine regulates cerebellar LTD and motor coordination through the delta2 glutamate receptor. *Nat. Neurosci.* **2011**, *14*, 603–611.

10. Jardon, B.; Bonaventure, N. N-Methyl-D-aspartate antagonists suppress the development of frog symmetric monocular optokynetic nystagmus observed after unilateral visual deprivation. *Brain Res. Dev. Brain Res.* **1992**, *67*, 67–73.
11. Godaux, E.; Cheron, G.; Mettens, P. Ketamine induces failure of the oculomotor neural integrator in the cat. *Neurosci. Lett.* **1990**, *116*, 162–167.
12. Mettens, P.; Cheron, G.; Godaux, E. NMDA receptors are involved in temporal integration in the oculomotor system of the cat. *Neuroreport* **1994**, *5*, 1333–1336.
13. Huang, Y.J.; Lin, C.H.; Lane, H.Y.; Tsai, G.E. NMDA Neurotransmission Dysfunction in Behavioral and Psychological Symptoms of Alzheimer's Disease. *Curr. Neuropharmacol.* **2012**, *10*, 272–285.
14. Puangthong, U.; Hsiung, G.Y. Critical appraisal of the long-term impact of memantine in treatment of moderate to severe Alzheimer's disease. *Neuropsychiatr. Dis. Treat.* **2009**, *5*, 553–561.
15. Utine, G.E.; Haliloglu, G.; Salanci, B.; Cetinkaya, A.; Kiper, P.O.; Alanay, Y.; Aktas, D.; Boduroglu, K.; Alikasifoglu, M. A Homozygous Deletion in GRID2 Causes a Human Phenotype With Cerebellar Ataxia and Atrophy. *J. Child Neurol.* **2013**, *28*, 926–932.
16. Maier, A.; Klopocki, E.; Horn, D.; Tzschach, A.; Holm, T.; Meyer, R.; Meyer, T. *De novo* partial deletion in GRID2 presenting with complicated spastic paraplegia. *Muscle Nerve* **2014**, *49*, 289–292.
17. Hills, L.B.; Masri, A.; Konno, K.; Kakegawa, W.; Lam, A.T.; Lim-Melia, E.; Chandy, N.; Hill, R.S.; Partlow, J.N.; Al-Saffar, M.; *et al.* Deletions in GRID2 lead to a recessive syndrome of cerebellar ataxia and tonic upgaze in humans. *Neurology* **2013**, *81*, 1378–1386.
18. Van Schil, K.; Meire, F.; Karlstetter, M.; Bauwens, M.; Verdin, H.; Coppieters, F.; Scheiffert, E.; van Nechel, C.; Langmann, T.; Deconinck, N.; *et al.* Early-onset autosomal recessive cerebellar ataxia associated with retinal dystrophy: New human hotfoot phenotype caused by homozygous GRID2 deletion. *Genet. Med.* **2014**, doi:10.1038/gim.2014.95.
19. Uebi, T.; Itoh, Y.; Hatano, O.; Kumagai, A.; Sanosaka, M.; Sasaki, T.; Sasagawa, S.; Doi, J.; Tatsumi, K.; Mitamura, K.; *et al.* Involvement of SIK3 in glucose and lipid homeostasis in mice. *PLOS ONE* **2012**, *7*, e37803.
20. Hemmings, H.C., Jr.; Yan, W.; Westphalen, R.I.; Ryan, T.A. The general anesthetic isoflurane depresses synaptic vesicle exocytosis. *Mol. Pharmacol.* **2005**, *67*, 1591–1599.
21. Rammes, G.; Danysz, W.; Parsons, C.G. Pharmacodynamics of memantine: An update. *Curr. Neuropharmacol.* **2008**, *6*, 55–78.
22. Seeman, P.; Caruso, C.; Lasaga, M. Memantine agonist action at dopamine D2High receptors. *Synapse* **2008**, *62*, 149–153.
23. Lee, J.W.; Park, H.J.; Choi, J.; Park, S.J.; Kang, H.; Kim, E.G. Comparison of ramosetron's and ondansetron's preventive anti-emetic effects in highly susceptible patients undergoing abdominal hysterectomy. *Korean J. Anesthesiol.* **2011**, *61*, 488–492.
24. Khojasteh, A.; Sartiano, G.; Tapazoglou, E.; Lester, E.; Gandara, D.; Bernard, S.; Finn, A. Ondansetron for the prevention of emesis induced by high-dose cisplatin. A multi-center dose-response study. *Cancer* **1990**, *66*, 1101–1105.
25. Jayadev, S.; Bird, T.D. Hereditary ataxias: Overview. *Genet. Med.* **2013**, *15*, 673–683.

26. Requena, T.; Espinosa-Sanchez, J.M.; Lopez-Escamez, J.A. Genetics of dizziness: Cerebellar and vestibular disorders. *Curr. Opin. Neurol.* **2014**, *27*, 98–104.
27. Rosini, F.; Federighi, P.; Pretegiani, E.; Piu, P.; Leigh, R.J.; Serra, A.; Federico, A.; Rufa, A. Ocular-motor profile and effects of memantine in a familial form of adult cerebellar ataxia with slow saccades and square wave saccadic intrusions. *PLOS ONE* **2013**, *8*, e69522.
28. Shirai, Y.; Asano, K.; Takegoshi, Y.; Uchiyama, S.; Nonobe, Y.; Tabata, T. A simple machine vision-driven system for measuring optokinetic reflex in small animals. *J. Physiol. Sci.* **2013**, *63*, 395–399.
29. Shutoh, F.; Ohki, M.; Kitazawa, H.; Itohara, S.; Nagao, S. Memory trace of motor learning shifts transsynaptically from cerebellar cortex to nuclei for consolidation. *Neuroscience* **2006**, *139*, 767–777.
30. Zuo, J.; de Jager, P.L.; Takahashi, K.A.; Jiang, W.; Linden, D.J.; Heintz, N. Neurodegeneration in Lurcher mice caused by mutation in delta2 glutamate receptor gene. *Nature* **1997**, *388*, 769–773.
31. Wang, Y.; Matsuda, S.; Drews, V.; Torashima, T.; Meisler, M.H.; Yuzaki, M. A hot spot for hotfoot mutations in the gene encoding the delta2 glutamate receptor. *Eur. J. Neurosci.* **2003**, *17*, 1581–1590.
32. Cull-Candy, S.G.; Wyllie, D.J. Glutamate-receptor channels in mammalian glial cells. *Ann. N. Y. Acad. Sci.* **1991**, *633*, 458–474.
33. Kato, A.S.; Knierman, M.D.; Siuda, E.R.; Isaac, J.T.; Nisenbaum, E.S.; Bredt, D.S. Glutamate receptor delta2 associates with metabotropic glutamate receptor 1 (mGluR1), protein kinase Cgamma, and canonical transient receptor potential 3 and regulates mGluR1-mediated synaptic transmission in cerebellar Purkinje neurons. *J. Neurosci.* **2012**, *32*, 15296–15308.
34. Hirai, H.; Launey, T.; Mikawa, S.; Torashima, T.; Yanagihara, D.; Kasaura, T.; Miyamoto, A.; Yuzaki, M. New role of delta2-glutamate receptors in AMPA receptor trafficking and cerebellar function. *Nat. Neurosci.* **2003**, *6*, 869–876.
35. Yamasaki, M.; Miyazaki, T.; Azechi, H.; Abe, M.; Natsume, R.; Hagiwara, T.; Aiba, A.; Mishina, M.; Sakimura, K.; Watanabe, M. Glutamate receptor delta2 is essential for input pathway-dependent regulation of synaptic AMPAR contents in cerebellar Purkinje cells. *J. Neurosci.* **2011**, *31*, 3362–3374.
36. Honore, T.; Davies, S.N.; Drejer, J.; Fletcher, E.J.; Jacobsen, P.; Lodge, D.; Nielsen, F.E. Quinoxalinediones: Potent competitive non-NMDA glutamate receptor antagonists. *Science* **1988**, *241*, 701–703.
37. Kakegawa, W.; Miyazaki, T.; Kohda, K.; Matsuda, K.; Emi, K.; Motohashi, J.; Watanabe, M.; Yuzaki, M. The N-terminal domain of GluD2 (GluRdelta2) recruits presynaptic terminals and regulates synaptogenesis in the cerebellum *in vivo*. *J. Neurosci.* **2009**, *29*, 5738–5748.
38. Rabacchi, S.; Bailly, Y.; Delhaye-Bouchaud, N.; Mariani, J. Involvement of the N-methyl D-aspartate (NMDA) receptor in synapse elimination during cerebellar development. *Science* **1992**, *256*, 1823–1825.
39. Garthwaite, J.; Brodbelt, A.R. Synaptic activation of N-methyl-D-aspartate and non-N-methyl-D-aspartate receptors in the mossy fibre pathway in adult and immature rat cerebellar slices. *Neuroscience* **1989**, *29*, 401–412.

40. Yuzaki, M.; Forrest, D.; Verselis, L.M.; Sun, S.C.; Curran, T.; Connor, J.A. Functional NMDA receptors are transiently active and support the survival of Purkinje cells in culture. *J. Neurosci.* **1996**, *16*, 4651–4661.
41. Balazs, R.; Jorgensen, O.S.; Hack, N. N-Methyl-D-aspartate promotes the survival of cerebellar granule cells in culture. *Neuroscience* **1988**, *27*, 437–451.
42. Ortega, F.; Perez-Sen, R.; Morente, V.; Delicado, E.G.; Miras-Portugal, M.T. P2X7, NMDA and BDNF receptors converge on GSK3 phosphorylation and cooperate to promote survival in cerebellar granule neurons. *Cell. Mol. Life Sci.* **2010**, *67*, 1723–1733.
43. Kadotani, H.; Hirano, T.; Masugi, M.; Nakamura, K.; Nakao, K.; Katsuki, M.; Nakanishi, S. Motor discoordination results from combined gene disruption of the NMDA receptor NR2A and NR2C subunits, but not from single disruption of the NR2A or NR2C subunit. *J. Neurosci.* **1996**, *16*, 7859–7867.
44. Marmolino, D.; Manto, M. Past, present and future therapeutics for cerebellar ataxias. *Curr. Neuropharmacol.* **2010**, *8*, 41–61.
45. Bormann, J. Memantine is a potent blocker of N-methyl-D-aspartate (NMDA) receptor channels. *Eur. J. Pharmacol.* **1989**, *166*, 591–592.
46. Strupp, M.; Brandt, T. Current treatment of vestibular, ocular motor disorders and nystagmus. *Ther. Adv. Neurol. Disord.* **2009**, *2*, 223–239.
47. Yoshida, T.; Katoh, A.; Ohtsuki, G.; Mishina, M.; Hirano, T. Oscillating Purkinje neuron activity causing involuntary eye movement in a mutant mouse deficient in the glutamate receptor delta2 subunit. *J. Neurosci.* **2004**, *24*, 2440–2448.
48. Faulstich, M.; van Alphen, A.M.; Luo, C.; du Lac, S.; De Zeeuw, C.I. Oculomotor plasticity during vestibular compensation does not depend on cerebellar LTD. *J. Neurophysiol.* **2006**, *96*, 1187–1195.
49. Gordon, J.W.; Uehlinger, J.; Dayani, N.; Talansky, B.E.; Gordon, M.; Rudomen, G.S.; Neumann, P.E. Analysis of the hotfoot (ho) locus by creation of an insertional mutation in a transgenic mouse. *Dev. Biol.* **1990**, *137*, 349–358.
50. Kashiwabuchi, N.; Ikeda, K.; Araki, K.; Hirano, T.; Shibuki, K.; Takayama, C.; Inoue, Y.; Kutsuwada, T.; Yagi, T.; Kang, Y.; *et al.* Impairment of motor coordination, Purkinje cell synapse formation, and cerebellar long-term depression in GluR delta 2 mutant mice. *Cell* **1995**, *81*, 245–252.
51. Wilson, D.B. Brain abnormalities in the lurcher (Lc) mutant mouse. *Experientia* **1975**, *31*, 220–221.
52. Nishiyama, J.; Matsuda, K.; Kakegawa, W.; Yamada, N.; Motohashi, J.; Mizushima, N.; Yuzaki, M. Reevaluation of neurodegeneration in lurcher mice: Constitutive ion fluxes cause cell death with, not by, autophagy. *J. Neurosci.* **2010**, *30*, 2177–2187.
53. Cendelin, J.; Tuma, J.; Korelusova, I.; Vozeh, F. The effect of genetic background on behavioral manifestation of Grid2(Lc) mutation. *Behav. Brain Res.* **2014**, *271*, 218–227.
54. Schwartz, E.J.; Rothman, J.S.; Dugue, G.P.; Diana, M.; Rousseau, C.; Silver, R.A.; Dieudonne, S. NMDA receptors with incomplete Mg(2)(+) block enable low-frequency transmission through the cerebellar cortex. *J. Neurosci.* **2012**, *32*, 6878–6893.
55. Hepp, R.; Hay, Y.A.; Aguado, C.; Lujan, R.; Dauphinot, L.; Potier, M.C.; Nomura, S.; Poirel, O.; El Mestikawy, S.; Lambolez, B.; *et al.* Glutamate receptors of the delta family are widely expressed in the adult brain. *Brain Struct. Funct.* **2014**, doi:10.1007/s00429-014-0827-4.

56. Glitsch, M.D. Calcium influx through N-methyl-D-aspartate receptors triggers GABA release at interneuron-Purkinje cell synapse in rat cerebellum. *Neuroscience* **2008**, *151*, 403–409.
57. Liu, S.J. Biphasic modulation of GABA release from stellate cells by glutamatergic receptor subtypes. *J. Neurophysiol.* **2007**, *98*, 550–556.
58. Duguid, I.C.; Smart, T.G. Retrograde activation of presynaptic NMDA receptors enhances GABA release at cerebellar interneuron-Purkinje cell synapses. *Nat. Neurosci.* **2004**, *7*, 525–533.
59. Hirano, T.; Watanabe, D.; Kawaguchi, S.Y.; Pastan, I.; Nakanishi, S. Roles of inhibitory interneurons in the cerebellar cortex. *Ann. N. Y. Acad. Sci.* **2002**, *978*, 405–412.
60. Whittingham, D.G. Fertilization of mouse eggs *in vitro*. *Nature* **1968**, *220*, 592–593.
61. Tabata, T.; Sawada, S.; Araki, K.; Bono, Y.; Furuya, S.; Kano, M. A reliable method for culture of dissociated mouse cerebellar cells enriched for Purkinje neurons. *J. Neurosci. Methods* **2000**, *104*, 45–53.

Salt-inducible kinase 3 deficiency exacerbates lipopolysaccharide-induced endotoxin shock accompanied by increased levels of pro-inflammatory molecules in mice

Masato Sanosaka,[1] Minoru Fujimoto,[2] Tomoharu Ohkawara,[2] Takahiro Nagatake,[3] Yumi Itoh,[1] Mai Kagawa,[1] Ayako Kumagai,[1] Hiroyuki Fuchino,[4] Jun Kunisawa,[3] Tetsuji Naka[2] and Hiroshi Takemori[1]

[1]*Laboratory of Cell Signalling and Metabolic Disease, National Institute of Biomedical Innovation, Ibaraki, Osaka,* [2]*Laboratory of Immune Signalling, National Institute of Biomedical Innovation, Ibaraki, Osaka,* [3]*Laboratory of Vaccine Materials, National Institute of Biomedical Innovation, Ibaraki, Osaka, and* [4]*Research Centre for Medicinal Plant Resources, National Institute of Biomedical Innovation, Tsukuba, Ibaraki, Japan*

doi:10.1111/imm.12445
Received 25 July 2014; revised 14 January 2015; accepted 20 January 2015.
Correspondence: M. Sanosaka and H. Takemori, Laboratory of Cell Signalling and Metabolic Disease, National Institute of Biomedical Innovation (NIBIO), 7-6-8, Asagi, Saito, Ibaraki, Osaka 567-0085, Japan.
Emails: m-sanosaka@nibio.go.jp and takemori@nibio.go.jp
Senior author: Masato Sanosaka

Summary

Macrophages play important roles in the innate immune system during infection and systemic inflammation. When bacterial lipopolysaccharide (LPS) binds to Toll-like receptor 4 on macrophages, several signalling cascades co-operatively up-regulate gene expression of inflammatory molecules. The present study aimed to examine whether salt-inducible kinase [SIK, a member of the AMP-activated protein kinase (AMPK) family] could contribute to the regulation of immune signal not only in cultured macrophages, but also *in vivo*. LPS up-regulated SIK3 expression in murine RAW264.7 macrophages and exogenously over-expressed SIK3 negatively regulated the expression of inflammatory molecules [interleukin-6 (IL-6), nitric oxide (NO) and IL-12p40] in RAW264.7 macrophages. Conversely, these inflammatory molecule levels were up-regulated in SIK3-deficient thioglycollate-elicited peritoneal macrophages (TEPM), despite no impairment of the classical signalling cascades. Forced expression of SIK3 in SIK3-deficient TEPM suppressed the levels of the above-mentioned inflammatory molecules. LPS injection (10 mg/kg) led to the death of all SIK3-knockout (KO) mice within 48 hr after treatment, whereas only one mouse died in the SIK1-KO (n = 8), SIK2-KO (n = 9) and wild-type (n = 8 or 9) groups. In addition, SIK3-KO bone marrow transplantation increased LPS sensitivity of the recipient wild-type mice, which was accompanied by an increased level of circulating IL-6. These results suggest that SIK3 is a unique negative regulator that suppresses inflammatory molecule gene expression in LPS-stimulated macrophages.

Keywords: AMP-activated protein kinase; endotoxin shock; interleukin-12p40; interleukin-1β; interleukin-6; inducible nitric oxide synthase; macrophage; salt-inducible kinases; tumour necrosis factor-α

Introduction

Macrophages play a critical role in the innate immune system during infection and systemic inflammation.[1] They produce pro-inflammatory cytokines such as tumour necrosis factor-α (TNF-α), interleukin-6 (IL-6) and IL-12 through recognition of bacterial components via Toll-like receptors (TLRs). Lipopolysaccharide (LPS; a cell-wall component of Gram-negative bacteria) is the ligand for TLR4.[2,3] When LPS binds to TLR4, its adaptor protein, the myeloid differentiation factor (MyD)88, recruits and activates IL-1 receptor-associated kinase family proteins,[4,5] which is followed by the activation of the transforming growth factor-β-activated kinase 1 (TAK1). The active TAK then transmits the signal through different pathways such as those involving the IκB kinase (IKK) family (IκBα-nuclear factor-κB) and the mitogen-activated protein kinases [MAPKs: extracellular signal-regulated kinase (ERK), p38, and c-Jun N-terminal kinase (JNK)]. TAK1 phosphorylates MAPK kinases (MKKs) and induces the activation of MAPKs.[6–8]

These MyD88-dependent cascades are initiated at an immediate early phase. In contrast, interferon-β-producing cascades such as those involving the interferon

regulatory factor 3 (IRF3) and the signal transducer and activator of transcription (STAT1) are activated by the MyD88-independent and Toll interleukin receptor-domain-containing adapter-inducing interferon-β-dependent pathways, which contributes to the late activation of nuclear factor-κB.[3,4,9–11] The gene expression of nitric oxide (NO) synthase 2 (Nos2 or inducible NOS; iNOS), which produces the inflammatory mediator NO, is also induced by active STAT1.[12,13]

Macrophages produce not only pro-inflammatory cytokines, but also anti-inflammatory cytokines. Macrophages are classified into two types, according to their pro-inflammatory or anti-inflammatory functions, classically activated macrophages (M1 macrophages) and alternatively activated macrophages (M2 macrophages), respectively. M2 macrophages are further classified into M2a, M2b, M2c, M2d[14] and M2b macrophages (also called regulatory macrophages) and produce anti-inflammatory cytokines such as IL-10.[15]

Salt-inducible kinase (SIK) is a member of the AMP-activated protein kinase (AMPK) family and plays a role in the regulation of glucose and lipid metabolism.[16,17] SIKs regulate the expression of several genes via the cAMP response element-binding protein (CREB) and myocyte enhancer factor 2 (MEF-2) transcription factors. The former is inhibited by SIKs via the phosphorylation-dependent inactivation of CREB-regulated transcription co-activators (CRTCs), which are CREB-specific co-activators[18–20] and the latter is activated via phosphorylation-dependent inactivation of class IIa histone deacetylases (HDAC), which act as co-repressors for MEF-2.[21,22] Both CRTCs and class IIa HDACs are sensitive to the cAMP–protein kinase A and calcineurin (phosphatase) cascades in which protein kinase A inactivates SIKs and calcineurin reactivates CRTCs and class IIa HDACs.[19]

Recently, SIK inhibitors were reported to polarize macrophages toward the M2b type through IL-10 production in a CRTC3-dependent manner.[23,24] On the other hand, Yong Kim *et al.*[25] reported that SIK1 and SIK3 negatively regulate TLR4-mediated signalling through interruption of the TAK1-binding protein (TAB)2–TNF receptor-associated factor (TRAF)6 complex by the inhibition of ubiquitination-dependent TRAF6 degradation. These reports suggest that SIKs play important roles in the inflammation and innate immune systems in cultured macrophages. However, the involvement of SIKs in inflammation *in vivo*, except for that in liver inflammation, cholestasis and cholelithiasis in SIK3-knockout (KO) mice,[26] remains unclear.

Here, we found that SIK3-KO mice, but not SIK1-KO and SIK2-KO mice, were highly sensitive to LPS and that SIK3-deficient macrophages produced increased levels of the inflammatory molecules, iNOS, IL-6 and IL-12p40 without any significant difference in the classical immune cascades. Moreover, adoptive transfer of SIK3-KO-bone marrow (SIK3-KO-BM) to X-ray-irradiated wild-type (WT) mice also increased LPS sensitivity in these mice.

Materials and methods

Mice

Age- and sex-matched littermates of SIK1-KO (C57BL6/J × 129 background), SIK2-KO and SIK3-KO (C57BL6/J background) mice described previously[26–28] were used in this study. For bone marrow transplantation, 8-week-old male C57BL6/J mice (Japan SLC, Hamamatsu, Japan) were used. All animal experiments were conducted according to the institutional ethical guidelines for animal experimentation of the National Institute of Biomedical Innovation (approved as nos. DS20-56, DS24-41 and DS26-86).

Cell culture

The murine RAW264.7 monocytic/macrophage cell line was obtained from the American Type Culture Collection (Manassas, VA). The cells were cultured in RPMI-1640 medium (Wako, Osaka, Japan) supplemented with 10% heat-inactivated fetal bovine serum (FBS) (Life Technologies, Carlsbad, CA). The isolation of mouse thioglycollate-elicited peritoneal macrophages (TEPM) is described elsewhere.[29] Briefly, 10- to 16-week-old mice were injected with 2 ml of 4% (w/v) Brewer's thioglycollate medium (BD Biosciences, San Diego, CA). Three or four days after the injection, the mice were killed by cervical dislocation under deep anaesthesia with isoflurane and their peritoneal macrophages were harvested by lavage with ice-cold PBS. The lavage fluid was transferred into polypropylene tubes, centrifuged at 370 ***g*** for 10 min, and the peritoneal macrophages were seeded at a density of 5.0×10^5 cells/cm^2. The non-adherent cells were washed out twice with PBS warmed at 37° and then cultivated in 10% FBS/RPMI-1640.

Real-time quantitative reverse transcription PCR

Total RNA was prepared using the ReliaPrep™ RNA Cell Miniprep System (Promega, Madison, WI), according to the manufacturer's instructions. Complementary DNA was synthesized by reverse transcription (RT) of 1 μg of total RNA by using the ReverTra Ace® qPCR RT Kit (Toyobo, Osaka, Japan) and used for quantitative PCR. The primers used in this study are listed in the Supporting information (Table S1).

Lentiviral transduction of SIK3 in RAW264.7 cells

The stable RAW264.7 line that over-expressed SIK3 was transduced using the ViraPower™ HiPerform™

Promoterless Gateway® Expression System (Life Technologies), according to the manufacturer's protocol. Briefly, the mouse *Sik3* (mSIK3) open reading frame was amplified by PCR with primers containing attB1/2 sequences, and the PCR product was cloned into the pDONR221 plasmid with BP clonase (Life Technologies). The mSIK3 open reading frame and the cytomegalovirus (CMV) promoter that was cloned into the pENTR plasmid were transferred into the plenti6.4-R4R2-DEST plasmid for preparing the lentiviral vector through the LR reaction. pLP1, pLP2, pLP-VSVG and plenti6.4-CMV-mSIK3 or -LacZ (control) were transformed into 293FT cells using the calcium phosphate method.[30] After 72 hr of transformation, the supernatant containing lentiviruses was collected and viral particles were purified using the Lenti-X™ Concentrator (Clontech, Mountain View, CA), according to the manufacturer's protocol. RAW264.7 cells were infected with lentiviruses, and the infected cells were selected by 10 μg/ml blasticidin (Santa Cruz Inc., Santa Cruz, CA) for 10 days.

Adenoviral transduction of SIK3 in thioglycollate-elicited mouse peritoneal macrophages

Adenoviral expression vectors for Lac Z, human SIK3 (hSIK3)-WT, and hSIK3-K37M mutant (kinase inactive form) were previously described.[31] The amplified adenoviruses were purified using Fast-Trap® Virus Purification and Concentration Kit (Millipore, Billerica, MA) according to the manufacturer's protocol. Thioglycollate-elicited mouse peritoneal macrophages isolated from SIK3-KO or WT mice were infected with adenoviruses (at a multiplicity of infection of 250) for 1 hr. After infection, the cells were washed with serum-free RPMI-1640 medium twice and incubated with 5% FBS/RPMI-1640 for 2 days.

Western blotting

The cells were washed three times with ice-cold PBS and lysed with the 1 × SDS buffer (50 mM Tris–HCl, 10% glycerol, 2% SDS; pH 6.8) without bromophenol blue. After measurement of protein concentration using Bicinchoninic acid (BCA) Protein Assay reagents (Thermo Scientific, Waltham, MA), the lysates were diluted with a one-third volume of 3 × SDS buffer supplemented with 10% 2-mercaptoethanol and bromophenol blue and heated at 100° for 5 min. Proteins (5–15 μg) were separated by SDS–PAGE and electrophoretically transferred onto PVDF membranes. The membranes were blocked with the Blocking One solution (Nacalai Tesque, Kyoto, Japan) and incubated with the following antibodies at 4° overnight: anti-SIK3 (1 : 2000; as per the method described earlier[31]), anti-α/β-tubulin (1 : 3000; #2148), anti-phospho-IKKα/β (1 : 1000; #2697), anti-IKKα/β (1 : 2000; sc-7607), anti-phospho-IκBα (1 : 1000; #2859), anti-IκBα (1 : 1000; #4812), anti-phospho-ERK (1 : 2000; #4376), anti-ERK (1 : 2000; #4695), anti-phospho-p38 (1 : 2000; #9215), anti-p38 (1 : 2000; #9212), anti-phospho-JNK (1 : 1000; #9251), anti-JNK (1 : 1000; #9252), anti-iNOS (1 : 500; sc-7271), anti-phospho-(pY701)-STAT1 (1 : 2000; #7649), anti-STAT1 (1 : 3000; #9172), anti-phospho-IRF3 (1 : 1000; #4947), anti-IRF3 (1 : 1000; #4302), or anti-β-actin (1 : 1000; sc-47778). Except for anti-IKKα/β, anti-iNOS, and anti-β-actin antibodies, which were purchased from Santa Cruz Biotechnology, all other antibodies were purchased from Cell Signaling Technology (Danvers, MA). Next, the membranes were incubated with an anti-rabbit horseradish peroxidase-conjugated goat antibody (111-035-144; Jackson ImmunoResearch Laboratory, West Grove, PA) or an anti-mouse horseradish peroxidase-conjugated goat antibody (1 : 10 000; 115-035-166; Jackson Immuno Research Laboratory) for 1 hr. The Chemi-Lumi One Super solution (Nacalai Tesque) was used for the detection of immune complexes.

Bone marrow transplantation

Bone marrow cells were prepared from the femur, tibia, humerus and pelvis of WT or SIK3-KO mice. Recipient mice were irradiated with X-ray (7 Gy). The cells (1×10^7 cells/head) were intravenously injected in the tail vein of irradiated recipient mice. Eight weeks after the transplantation, the recipient mice were used for experiments.

LPS-induced endotoxin shock model

Lipopolysaccharide (10 mg/kg body weight; derived from O111 *Escherichia coli*; phenol-extracted, Wako) dissolved in PBS was injected intraperitoneally into 14-week-old mice. Blood was collected from a small cut on the tail, and serum was separated by centrifugation at 1000 ***g*** for 10 min, collected into tubes, and stored at −40° until analysis.

Measurement of cytokine production by ELISA

The cytokine levels in media containing LPS-stimulated mouse peritoneal macrophages or RAW264.7 cells were quantified by ELISA with the ELISA MAX™ Deluxe (BioLegend, San Diego, CA), as per the manufacturer's instructions. The cytokine levels were normalized to those of cellular protein measured by using the BCA Protein Assay Kit (Thermo Scientific).

Measurement of NO production

Griess reagent (0.05% naphthylethylenediamine dihydrochloride, 0.5% sulphonylamide and 2.5% phosphoric

acid) was prepared and stored at 4° in the dark. Media from LPS-stimulated mouse TEPM or RAW264.7 cells were collected into fresh tubes and then mixed with Griess reagent at a 1 : 1 ratio in a 96-well plate. Absorbance was measured spectrophotometrically at 550 nm. Concentration of NO was normalized to the cellular protein concentration measured by using the BCA Protein Assay Kit (Thermo Scientific).

Statistical analyses

For all experiments, data are expressed as mean ± standard error of the mean (SEM), with at least three repeats for each experimental group. Statistical analyses were performed using the Student's *t*-test or two-way analysis of variance followed by Bonferroni's post-tests for the comparison of gene expression and cytokine secretion. The Cox–Mantel test was used to analyse the Kaplan–Meier curve for mouse survival.

Results

Increase in SIK3 mRNA level after LPS treatment in RAW264.7 macrophages

According to recent studies using SIK inhibitors and RNA interference techniques,[23,25] all SIK isoforms contribute to inflammatory responses in macrophages. However, information regarding the expression of each SIK isoform in macrophages is limited. To measure the expression of SIK family kinases in macrophages, RAW264.7 cells were stimulated with LPS (Fig. 1). Sixteen hours after LPS treatment, the mRNA level of SIK3, but not SIK1 or SIK2, was significantly up-regulated in RAW264.7 macrophages treated with 10, 100 and 1000 ng/ml LPS (Fig. 1a). We also examined the time-dependent change of SIK isoform mRNA levels after LPS (100 ng/ml) stimulation (Fig. 1b). The SIK3 mRNA level hovered at a high level of expression compared with that observed in the control (only medium replacement), from 4 to 16 hr after LPS stimulation. A small, or less, difference in SIK1 or SIK2 mRNA level was observed between LPS stimulation and control (two-way analysis of variance followed by Bonferroni's post-test suggested a significance in SIK2 mRNA at the 4 hr-point).

SIK3 over-expression suppresses inflammatory molecule expression

To examine whether the different level of SIK3 expression affects the levels of pro-inflammatory or anti-inflammatory molecules after LPS stimulation, we prepared mouse SIK3 (mSIK3) over-expressing RAW264.7 macrophages using lentiviruses. Western blotting revealed that SIK3 protein level in mSIK3 over-expressing cells was higher than that in the control cells (Lac Z) (Fig. 2a). Suppressed mRNA levels of IL-6, iNOS and IL-12p40 were observed after LPS stimulation (Fig. 2b). However, no significant difference in TNF-α and IL-1β mRNA levels was observed between the control and mSIK3 over-expressing cells. On the other hand, 1 hr after LPS stimulation, IL-10 mRNA levels were also lower in mSIK3 over-expressed RAW264.7 macrophages than in LacZ-control.

SIK3-deficient macrophages produce high levels of inflammatory molecules

Next, we examined the effects of SIK3 deficiency on the levels of inflammatory molecules. Because the RNA interference technique was not successful for SIK3 in our laboratory, we prepared TEPM from SIK3-KO and WT mice. In contrast to the findings in mSIK3 over-expressed RAW264.7 macrophages, after 4 hr of LPS stimulation, the mRNA levels of IL-6, iNOS and IL-12p40 were higher in SIK3-KO TEPM than in WT TEPM (Fig. 3a). In addition, no significant difference was observed in TNF-α or IL-1β expression levels between SIK3-KO and WT TEPM. These results suggested that the molecules whose expression was regulated by SIK3 are restricted to the secondary genes that were not fully induced at 1 hr after LPS stimulation. On the other hand, IL-10 mRNA level was also higher in SIK3-KO TEPM than in WT TEPM at 1 hr after LPS stimulation, suggesting that the increase in the expression of secondary genes in SIK3-KO TEPM might be out of the control of, or independent of, the IL-10 altered expression.

In addition to mRNA quantification, we measured the production of cytokines (IL-6, TNF-α and IL-10) and NO in SIK3-KO TEPM (Fig. 3b,c). After stimulation with LPS, SIK3-KO TEPM produced higher IL-6 (twofold, Fig. 3b left panel) and NO (3.5-fold, Fig. 3c) levels than WT TEPM. In contrast, TNF-α production in SIK3-KO TEPM was lower than that in WT TEPM (Fig. 3b middle panel). Interleukin-10 production was also slightly, but clearly, higher in SIK3-KO TEPM than in WT TEPM (Fig. 3b right panel). Furthermore, adenovirus-mediated SIK3 reconstitution in the SIK3-KO TEPM lowered IL-6 production to the level observed in WT TEPM (Fig. 3d, e), which was not observed when a kinase-defective SIK3 (K37M mutant) was reconstituted.

The completeness of signalling cascades in the induction of inflammatory molecules was confirmed by Western blotting (Fig. 3f, classified into the primary response). No significant difference was observed in IKK, IκBα and MAPK phosphorylation levels between WT and SIK3-KO TEPM after LPS stimulation. However, the JNK protein total level was lower in SIK3-KO TEPM than in WT TEPM, but phosphorylated JNK levels did not differ in these macrophages. In addition to these primary

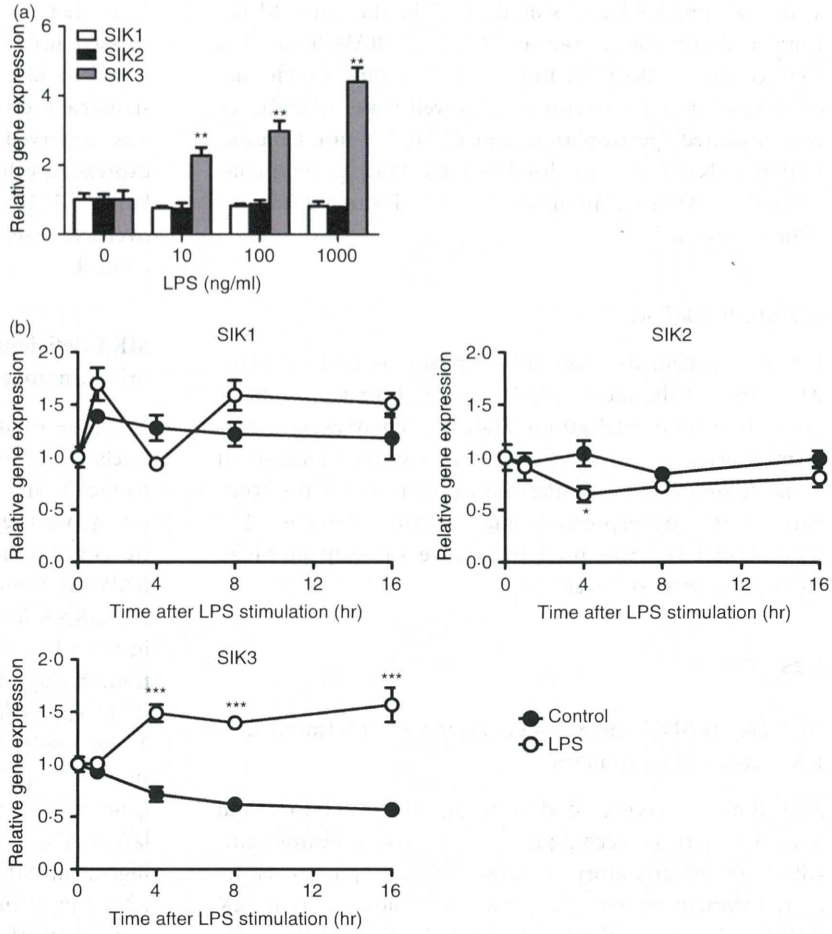

Figure 1. Salt-inducible kinase (SIK) family kinase gene expression levels in RAW264.7 cells after lipopolysaccharide (LPS) treatment. (a) RAW264.7 cells (1.5×10^5 cells/cm^2) were stimulated with the indicated dose of LPS for 16 hr. (b) RAW264.7 cells were stimulated with 100 ng/ml LPS and harvested at the indicated time-points. After total RNA isolation, the mRNA levels of SIK1, SIK2 and SIK3 were analysed by quantitative PCR. Hypoxanthine-guanine phosphoribosyltransferase (HPRT) was used as an internal control. The data are expressed as mean ± SEM ($n = 3$). Statistical analyses were performed using the Student's *t*-test (a) or two-way analysis of variance followed by Bonferroni's post-tests (b) for the comparison of gene expression. $*P < 0.05$, $**P < 0.01$, $***P < 0.001$.

response cascades, phosphorylation levels of secondary response signal transducers such as IRF3 and STAT1 also did not differ in macrophages (Fig. 3g).

In addition to SIK3-KO TEPM experiments, we prepared TEPM from SIK1-KO and SIK2-KO mice and quantified pro-inflammatory and anti-inflammatory molecule mRNA expression (see Supporting information, Fig. S1). Notably, IL-10 mRNA level was down-regulated in SIK1-KO macrophages at 1 hr after LPS stimulation (Fig. S1a), whereas it was up-regulated in SIK2-KO macrophages (Fig. S1b). Although statistical analyses showed some differences in other gene expression levels between WT and SIK1-KO or SIK2-KO TEPM, these differences (especially in the levels of secondary genes) were smaller than those between SIK3-KO TEPM and its control WT TEPM (Fig. 3a).

To argue about the nature of macrophages in SIK3 signalling, we assessed the expression of pro-inflammatory and anti-inflammatory molecules in bone marrow-derived macrophages (BMDM) prepared from WT or SIK3-KO mice (see Supporting information, Fig. S2). Consistent with the results of TEPM, significant differences in IL-6 and iNOS mRNA levels between SIK3-KO and WT BMDM were observed at 4 hr after LPS stimulation. Furthermore, IL-12p40 mRNA was higher in SIK3-KO BMDM than in WT BMDM. Lower TNF-α levels and higher IL-10 levels in SIK3-KO BMDM than in WT BMDM were observed at 1 hr after LPS stimulation.

SIK3 deficiency exacerbates endotoxin shock in mice

The absence of SIK3 resulted in enhanced mRNA levels of the inflammatory molecules categorized as secondary genes. To examine the importance of SIK3 in the regulation of LPS-induced endotoxin shock *in vivo*, SIK1-3-KO mice were intraperitoneally injected with 10 mg/kg of LPS (Fig. 4a). All SIK3-KO mice died within 48 hr of LPS injection, whereas only one mouse died in the SIK1-KO, SIK2-KO and control groups (WT, both C57BL/6 and C57BL/6 × 129 genetic backgrounds). Serum IL-6 levels in WT, SIK1-KO and SIK2-KO mice rapidly increased after LPS treatment, reached a peak at 2–4 hr, and then decreased (Fig. 4b). However, a continuous increase in the serum IL-6 level in SIK3-KO mice was observed until 8 hr after LPS treatment. In all mouse groups, serum TNF-α levels rapidly reached a peak 1 hr after LPS treatment (Fig. 4c). Decreased serum TNF-α level in SIK2-KO and SIK3-KO mice was observed. These